18. Cookson MS, Aus G, Burnett AL, Canby-Hagino ED, D'Amico AV, Dmochowski RR, Eton DT, Forman JD, Goldenberg SL, Hernandez J, Higano CS, Kraus SR, Moul JW, Tangen C, Thrasher JB, Thompson I. Variation in the definition of biochemical recurrence in patients treated for localized prostate cancer: The American Urological Association Prostate Guidelines for Localized Prostate Cancer Update Panel report and recommendations for a standard in the reporting of surgical outcomes. J Urol 2007;177(2):540–545.
19. Greene FL, Sobin LH. A worldwide approach to the TNM staging system: Collaborative efforts of the AJCC and UICC. J Surg Oncol 2009;99(5):269–272.
20. Ryo A, Uemura H, Ishiguro H, Saitoh T, Yamaguchi A, Perrem K, Kubota Y, Lu KP, Aoki I. Stable suppression of tumorigenicity by Pin1-targeted RNA interference in prostate cancer. Clin Cancer Res 2005;11(20):7523–7531.
21. Miranda C, Roccato E, Raho G, Pagliardini S, Pierotti MA, Greco A . The TFG protein, involved in oncogenic rearrangements, interacts with TANK and NEMO, two proteins involved in the NF-kappaB pathway. J Cell Physiol 2006;208(1):154–160.
22. Ayala G, Wang D, Wulf G, Frolov A, Li R, Sowadski J, Wheeler TM, Lu KP, Bao L. The prolyl isomerase Pin1 is a novel prognostic marker in human prostate cancer. Cancer Res 2003; 63(19):6244–6251.
23. Sasaki T, Ryo A, Uemura H, Ishiguro H, Inayama Y, Yamanaka S, Kubota Y, Nagashima Y, Harada M, Aoki I. An immunohistochemical scoring system of prolyl isomerase Pin1 for predicting relapse of prostate carcinoma after radical prostatectomy. Pathol Res Pract 2006;202(5):357–364.
24. Frater-Schroder M, Risau W, Hallmann R, Gautschi P, Bohlen P. Tumor necrosis factor type alpha, a potent inhibitor of endothelial cell growth in vitro, is angiogenic in vivo. Proc Natl Acad Sci USA 1987;84(15):5277–5281.
25. Xu X, Fu XY, Plate J, Chong AS. IFN-gamma induces cell growth inhibition by Fas-mediated apoptosis: requirement of STAT1 protein for up-regulation of Fas and FasL expression. Cancer Res 1998;58(13):2832–2837.

the FEBS Journal
REVIEW ARTICLE

Mass spectrometric characterization of proteins transferred from polyacrylamide gels to membrane filters

Yoko Ino and Hisashi Hirano

Advanced Medical Research Center/Graduate School of Nanobioscience, Yokohama City University, Japan

Keywords
electroblotting; gel electrophoresis; mass spectrometry (MS); protein

Correspondence
H. Hirano, Yokohama City University, Advanced Medical Research Center, Fukuura 3-9, Kanazawa, Yokohama 236-0004, Japan
Fax: +81 45 787 2787
Tel: +81 45 787 2791
E-mail: hirano@yokohama-cu.ac.jp

(Received 2 April 2011, revised 1 August 2011, accepted 11 August 2011)

doi:10.1111/j.1742-4658.2011.08303.x

In the 1990s, a technique was developed to transfer proteins from electrophoresis gels onto poly(vinylidene difluoride) (PVDF) membranes, digest the proteins on the membranes with proteases such as trypsin and analyze the resulting peptides on the membranes directly by mass spectrometry to identify the proteins. This technique, based on gel electrophoresis, is particularly useful for analyzing protein isoforms, splicing variants and post-translationally modified proteins. Previously, the low ionization efficiency of peptides immobilized on the membranes often rendered this technique useless. However, this technique has been improved by the use of PVDF membranes with a small pore size, which has enabled highly efficient and effective electroblotting and mass spectrometric analyses. Here, the advantage of this technique is discussed.

Proteomic analyses begin with protein expression profiling

Proteome research involves the comprehensive analysis of protein expression profiles, the function and functional networks of proteins, and the relationship between proteins and diseases. Upgraded protein databases, and highly sensitive, accurate and high-throughput analytical techniques, such as mass spectrometry (MS), have greatly facilitated and accelerated the development of proteome research.

Two standard methods, the protein shotgun method [1] and the 2D electrophoresis (2DE)-MS/MS method [2], are commonly used in the first step of proteome analysis. In the shotgun method, a sample containing a number of proteins is digested with proteases such as trypsin, which has comparatively high substrate specificity. These digested proteins are separated by liquid chromatography (LC), analyzed by MS/MS and then identified based on their sequence information. In contrast, in the 2DE-MS/MS method, most proteins are separated by 2DE, protease-digested in gels and then analyzed by MS [3]. Next, the proteins are identified based on peptide mass fingerprints or on sequence information obtained by MS/MS and database searches [4].

Both methods can profile the expression of a number of proteins. However, the shotgun method has been more frequently used for recent proteomic analyses. The shotgun method typically identifies more proteins than 2DE-MS/MS. In addition, the shotgun method can be easily automated and therefore does not require professional skills for the analysis. In contrast, 2DE is laborious, and it is not easy for beginners to obtain reproducible results, particularly with the 'in-gel' digestion of proteins after electrophoresis. However, the shotgun method cannot completely replace 2DE-MS/MS for proteomic studies because 2DE-MS/MS has several advantages over the shotgun method, as described below.

Advantages of gel electrophoresis

The resolution of MS, using techniques such as matrix-assisted laser dissociation ionization-time-of-flight (MALDI-TOF)/TOF MS, electrospray ionization-quadrupole (ESI-Q)/TOF MS, ESI-linear ion trap (LIT)/TOF MS and even LTQ-Orbitrap MS, is often insufficient to measure directly the precise masses of high-molecular-weight proteins. Therefore, proteins must be digested with proteases to obtain peptides that can be analyzed using these MS approaches. Accordingly, this method often misses information on protein isoforms, splicing variants and post-translational modifications, which might be obtained by analyzing intact proteins. In contrast, electrophoresis, particularly 2DE using IEF in the first dimension and sodium dodecyl sulfate-polyacrylamide gel electrophoresis (SDS/PAGE) in the second dimension [5,6], can easily separate isoforms, splicing variants and post-translationally modified proteins. Jungblut *et al.* [7] pointed out that there are many isoforms and post-translationally modified proteins, and advocated that these protein species are a secondary component of the proteome. They noted that some proteins have tens of isoforms, including post-translationally modified proteins. These proteins can be separated by gel electrophoresis and identified by MS analysis, while it is not easy to identify these protein species using the shotgun method.

There are several useful electrophoresis techniques in addition to O'Farrell's 2DE. For example, 2DE using Phos-tag gel electrophoresis [8] instead of SDS/PAGE in the second dimension is suitable for analyzing the phosphorylation status of phosphoproteins, which is impossible to perform using the shotgun method [9]. 2DE using blue native electrophoresis in the first dimension and SDS/PAGE in the second dimension can separate proteins within a protein complex and identify the complex components by MS [10].

In addition, a protein differential display technique using gel electrophoresis – 2D difference gel electrophoresis (2D-DIGE) – has recently been developed [11]. This technique is particularly useful for identifying disease-associated proteins [12] and post-translationally modified proteins [13].

Benefits of poly(vinylidene difluoride) membranes

Towbin *et al.* [14] established a western blotting technique in which proteins are separated by gel electrophoresis, electrophoretically transferred onto the appropriate membrane filters and then detected with specific antibodies. This method became widely used as a result of the high sensitivity of detection, simplicity of handling and use of straightforward techniques to desalt the samples and preserve the membranes. In addition, secondary antibodies and fluorescent reagents were recently applied to this technique, making the analysis even more sensitive and easier to perform.

Subsequently, this method was used to detect phosphoproteins [15], glycoproteins [16] and various ligand-binding proteins. At that time, nitrocellulose membranes were predominantly used for western blotting. In the 1980s, Y. Monji (Millipore, Osaka) found that poly(vinylidene difluoride) (PVDF) membranes could be used for western blotting. In those days, a novel protein sequencer, called a gas-phase sequencer, was rapidly developed that differed from previous sequencers. With the gas-phase sequencer, the purified protein was immobilized noncovalently on a small glass-fiber filter and then Edman degradation was performed on the filter. This development led to the idea that gel-resolved proteins could be transferred onto this glass-fiber filter by western blotting and sequenced using the gas-phase sequencer [17,18]. However, the blotting efficiency of the glass-fiber filter was insufficient, making this method impractical. Like the nitrocellulose membranes, the membrane filters could not be used with the sequencer because they were intolerant to the organic solvents used for Edman degradation. However, Matsudaira [19] found that PVDF membranes were suitable as a membrane filter for protein immobilization in gas-phase sequencing. Thus, PVDF membranes became widely used as a membrane filter for sequencing as well as western blotting.

Proteins blotted onto the membrane filters can be analyzed by MS

Since the 1980s, protein and peptide MS has developed rapidly. The sensitivity, accuracy and throughput have been improved by one digit per year. Presently, we can rapidly obtain information on amino acid sequences, post-translational modifications, and protein–protein interactions by MS analysis using only 1 fmol of the protein sample. In many cases, proteins are separated by 2DE, digested in gels and then identified by MS. However, this method is laborious and time consuming if an automated in-gel digestion instrument is not available. Moreover, sometimes the peptide yields are not reproducible. If proteins that are transferred from the electrophoresis gels to the membrane filters can be analyzed directly by MS, we can efficiently identify proteins on the membrane filters. For the MS analysis of proteins on membranes, it is unnecessary to perform in-gel digestion. We can analyze post-translational

modifications and protein–protein interactions simultaneously by MS analyses of the proteins on the membrane filters.

Identification of proteins on membranes

Since the 1990s, studies of proteins separated by gel electrophoresis, electroblotted and analyzed by MS have been performed. In brief, proteins resolved by SDS/PAGE were electroblotted onto Fluorotrans PVDF membranes, pieces of the membrane that contained proteins were cut out and the molecular masses of the proteins on membranes were measured using MALDI-MS [20]. Subsequently, proteins separated by SDS/PAGE were electroblotted onto five types of PVDF membranes – Transblot, Immobilon P^{SQ}, Fluorotrans, Westran S and Immobilon-P – and pieces of the membrane containing a protein of interest were incubated with the matrix, cut out and mounted on the sample support using conductive double-sided adhesive tape; then, the molecular mass values of proteins were determined by infrared (IR)-MALDI-TOF MS [21]. The authors described that in this experiment, better results were obtained from membranes that had highly specific surfaces and a low mean pore size. Similar studies were performed by several groups in order to determine the molecular mass values of gel-resolved proteins on membranes [22–24].

This technique was applied for identification of gel-resolved proteins using MALDI-MS. Patterson [25] digested gel-resolved proteins on PVDF membranes with Lys-C endopeptidase and eluted the digests from the membranes for analysis by MALDI-MS in order to identify the proteins. The author used Immobilon-CD PVDF membranes with quarternary amines linked to the membrane surface, which might be useful for efficient recovery of the electroblotted proteins (peptides) from the membranes. Later, several groups identified gel-resolved proteins using similar techniques, but different types of membranes, such as PVDF membranes (Problot and Hybond-P) and nitrocellulose [26–30].

In 1999, Schleuder *et al.* [31] digested gel-resolved proteins on membranes and analyzed the proteins on the membranes directly, using MALDI-MS. In brief, after digestion, they secured pieces of PVDF membrane containing the proteins onto the MALDI sample plate using conductive double-sided adhesive tape, and introduced it into the IR-MALDI-MS in order to identify the proteins by peptide mass fingerprinting. In this study, the best performance of IR-MALDI-MS was obtained using Immobilon-CD membrane, but no results were available for other PVDF membranes, such as Immobilon P^{SQ} and Transblot membranes. In this experiment, 0.1 μm pore-size and 195-μm-thick Immobilon P^{SQ} membranes (see Table 1 for the pore size of membranes) were used. The Immobilon-CD and 0.1 μm pore-size Immobilon P^{SQ} membranes are not currently available commercially. Therefore, we cannot repeat these experiments.

On-membrane characterization of gel-resolved proteins by MS

The gel-resolved proteins can be characterized by MALDI-MS. Sloane *et al.* [32] immobilized gel-resolved proteins onto Immobilon P^{SQ} PVDF and nitrocellulose membranes, and digested the proteins with proteases on membranes using a piezoelectric chemical inkjet printer, and then they identified antigens and glycoproteins using MS. Kimura *et al.* [33] and Nakanishi *et al.* [34,35] used the same piezoelectric chemical inkjet printer for the enzymatic digestion of proteins on membranes. Kimura *et al.* [33] electroblotted gel-resolved proteins onto Immobilon P^{SQ}

Table 1. Pore size of membrane filters described in this paper.

Membrane name	Membrane	Hydrophobicity	Pore size (μm)	Distributor
Fluorotrans	PVDF	Hydrophobic	0.2	Pall (Port Washington, NY, USA)
Hybond-P	PVDF	Hydrophobic	0.45	GE Healthcare (Uppsala, Sweden)
Immobilon-CD	PVDF	Hydrophilic	0.1	Millipore (Bedford, MA, USA)
Immobilon FL	PVDF	Hydrophobic	0.45	Millipore (Bedford, MA, USA)
Immobilon-P	PVDF	Hydrophobic	0.45	Millipore (Bedford, MA, USA)
Immobilon P^{SQ}	PVDF	Hydrophobic	0.2[a]	Millipore (Bedford, MA, USA)
0.1 μm pore-size PVDF	PVDF	Hydrophobic	0.1	Millipore (Bedford, MA, USA)
Problot	PVDF	Hydrophobic	0.2	Applied Biosystems (Foster City, CA, USA)
Transblot	PVDF	Hydrophobic	0.2	BioRad (Rockville, MD, USA)
Westran S	PVDF	Hydrophobic	0.2	GE Healthcare (Uppsala, Sweden)
Nitrocellulose	Nitrocellulose	Hydrophobic	0.45	–

[a] Before 1999, 0.1 μm pore-size Immobilon P^{SQ} membranes were available. The Immobilon P^{SQ} membrane is 195 μm thick; the other membranes are 140–150 μm thick [21].

membranes and used multiple proteases and PNGase F to identify the proteins and detect the *N*-linked glycans, respectively. Nakanishi *et al.* [35] identified tyrosine-phosphorylated proteins from *Escherichia coli* cells on Immobilon FL membranes using an anti-phosphotyrosine Ig. After on-membrane digestion, they identified the phosphoproteins using MALDI-TOF MS.

Chang *et al.* [29] separated membrane proteins from gram-negative bacteria by SDS/PAGE, electroblotted the proteins onto the Hybond-P PVDF membranes and then fixed the membrane to the sample target using conductive double-sided adhesive tape. The matrix for MALDI-TOF MS was added to the samples for MS analysis. Then, they successfully measured the molecular masses of the proteins with relative molecular mass values of 28,000-35,000. MS analysis revealed that a 28-kDa protein was *N*-acetylated.

Chen *et al.* [36] immobilized, on Hybond-P PVDF membrane, antibodies that were raised against three proteins and interacted with antigens in plasma samples. The PVDF membranes were attached to the sample plate using conductive double-sided adhesive tape and analyzed by MALDI-TOF MS. Chen *et al.* showed that this technique could be used to confirm the interaction between antigen and antibody, suggesting that it is possible to analyze various interactions between proteins and ligands.

Small pore size of membrane increases ion yield in MS

Thus, many interesting techniques have been developed that combine electrophoresis, blotting and MS. However, these techniques did not always yield strong and interpretable results. One of the reasons for this poor outcome is the low ionization efficiency or low ion yield of peptides and proteins that are immobilized on PVDF membranes. Therefore, it was necessary to develop new membranes on which digests of the immobilized protein can be ionized efficiently. Without this improvement, peptides obtained by on-membrane digestion of gel-resolved proteins would have to be eluted from the membrane and then subjected to MALDI for identification [25–30].

Previously, 0.2–0.45 μm pore-size PVDF membranes have been mainly used for electroblotting and subsequent

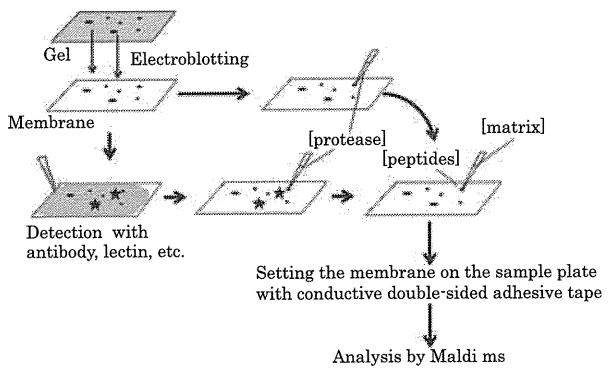

Fig. 1. Experimental procedure of MS analysis of proteins blotted from gels onto PVDF membranes.

Table 2. Recommended method for protein identification on membrane.

Immobilization of proteins onto membranes [39]
Proteins were separated by electrophoresis through a polyacrylamide gel
The polyacrylamide gel was soaked in 100 mL of 25 mM Tris/40 mM 2-amino-*n*-caproic acid buffer (pH 9.0) containing 20% (v/v) methanol (solution C) for 15 min with gentle shaking. This procedure was repeated twice
PVDF membranes were dipped in 100% methanol for 10 s and subsequently in Solution C for 15 min with shaking
200 mL of 0.3 M Tris (pH 10.5) containing 20% (v/v) methanol (Solution A), 200 mL of 25 mM Tris (pH 10.5) containing 20% (v/v) methanol (Solution B) and 200 mL of Solution C were poured into three separate stainless steel trays. Two pieces of Whatman 3MM filter paper were immersed into each solution in the trays and shaken gently for 10 min. The solution was replaced with fresh solution, and the filter papers were shaken for a further 10 min
After removal of the excess solution attached to the filters and gel, the filter paper, PVDF membrane and gel were assembled into a sandwich as follows: from the cathode side, (a) two filter papers saturated with Solution C, (b) PVDF membranes with Solution C, (c) gel equilibrated with Solution C, (d) two filter papers saturated with Solution B and (e) two filter papers saturated with Solution A. These were sandwiched between the cathode and anode electrode plates of the semidry blotting apparatus and the proteins were transferred from the gel to the membrane
The proteins blotted onto the PVDF membrane were detected by Direct Blue 71 staining or Ponceau-S staining
On-membrane tryptic digestion [34]
The membranes were rinsed with distilled water and affixed to a MALDI target plate using electrically conductive double-sided adhesive tape
An aliquot (0.5 μL) of the protease solution containing 100 $\mu g \cdot mL^{-1}$ of trypsin in 25 mM NH_4HCO_3 (pH 8.0)/40% (v/v) acetonitrile was spotted on each protein position
Proteins on the membranes were digested with trypsin overnight at 37°C in the reaction chamber with moisture
On-membrane MS analysis [34]
After the digestion, 0.5 μL of the matrix solution, which was saturated with α-cyano-4-hydroxycinnamic acid or 10 $mg \cdot mL^{-1}$ of 2,5-dihydroxybenzoic acid in 0.1% (v/v) trifluoroacetic acid/30% (v/v) acetonitrile, was spotted on the protein positions
The digests were analyzed using MALDI-TOF MS or MALDI-TOF/TOF MS

MS analysis of gel-resolved proteins (Fig. 1). Recently, membranes that might be suitable for this purpose were explored [37]. In this work, proteins separated by electrophoresis were immobilized on membranes, such as PVDF, poly(tetrafluoroethylene) (PTFE), poly(ethersulfone) (PES), nitrocellulose, polycarbonate and polypropylene, by electroblotting. Proteins were not transferred efficiently onto hydrophobic membranes such as PTFE, PES, polycarbonate and polypropylene. Among these various membrane filters, PVDF membranes exhibited the highest blotting efficiency. Moreover, the efficiency of the same PVDF membrane in MS varied depending on the pore size. Among 0.1, 0.22 and 0.45 μm pore-size PVDF membranes, the mass signal intensity was highest in 0.1 μm pore-size PVDF membranes, and a smaller pore size resulted in stronger mass signal intensity was greater than that of PVDF membranes with a 0.22 μm pore-size when the proteins were digested and measured on the membranes using MALDI-TOF MS (Table 2, Fig. 2). This 0.1 μm pore-size PVDF membrane is ~ 140 μm thick, and different from the old 195-μm-thick Immobilon PS^{Q} membrane, as described above.

As a trial, yeast proteins were separated by 2DE and blotted onto 0.1 μm pore-size PVDF membranes. Among hundreds of blotted proteins, 19 were selected, including high-abundance and low-abundance proteins, high-molecular-weight and low-molecular-weight proteins, and basic and acidic proteins (Fig. 3), for protein identification. After digesting these proteins with trypsin, the digests were analyzed on membranes by MALDI-TOF/TOF MS, and all 19 proteins were successfully identified. It was possible to identify comprehensively many proteins from yeast, as described previously [37].

It is likely that proteins cannot penetrate very small pores during electroblotting, and most of the proteins may be retained on the surface of the membrane in the case of 0.1 μm pore-size membranes. On the other hand, peptides generated by tryptic digestion may not easily spread into membranes with a small pore size. Proteins and peptides on the membrane surface are easily irradiated by lasers, resulting in increased ion yield. Furthermore, PVDF membranes with a pore size of 0.1 μm could prevent the diffusion of the matrix solution that was added to the samples.

Iwafune *et al.* [38] previously developed a diamond-like carbon-coated stainless steel (DLC) plate that was chemically modified with an *N*-hydroxysuccinimide ester. This ester reacts with primary amines on proteins and covalently attaches them to the surface of the DLC plate. Because the DLC plate is conductive, it can be used to electroblot proteins from gels following gel electrophoresis. Moreover, this plate can be used as a target plate for MALDI-TOF MS. Using the DLC plate and MALDI-TOF MS, protein digestion on the DLC plate and peptide mass fingerprinting analyses were performed to identify proteins. However, special devices are required to electroblot the proteins from the gels onto the DLC plate. For example, 0.3-mm-thick SDS-polyacrylamide gels must be used to increase the blotting efficiency, and the gels handled carefully after electrophoresis. In addition, the DLC plates are very expensive because they require

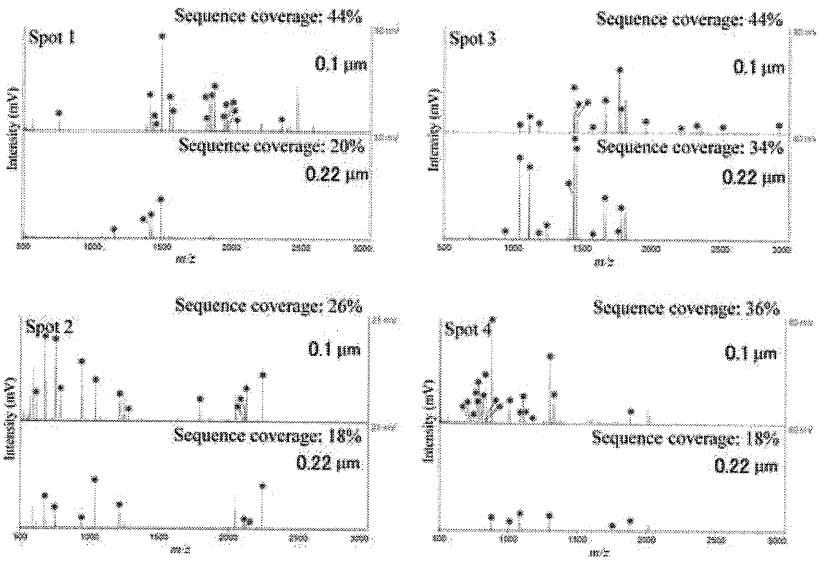

Fig. 2. Mass spectra of yeast proteins that were separated by 2DE and then electroblotted onto PVDF membranes with different pore sizes. Spots 1–4, as shown in Fig. 3, were analyzed using MALDI-quadrupole ion trap (QIT)/TOF MS.

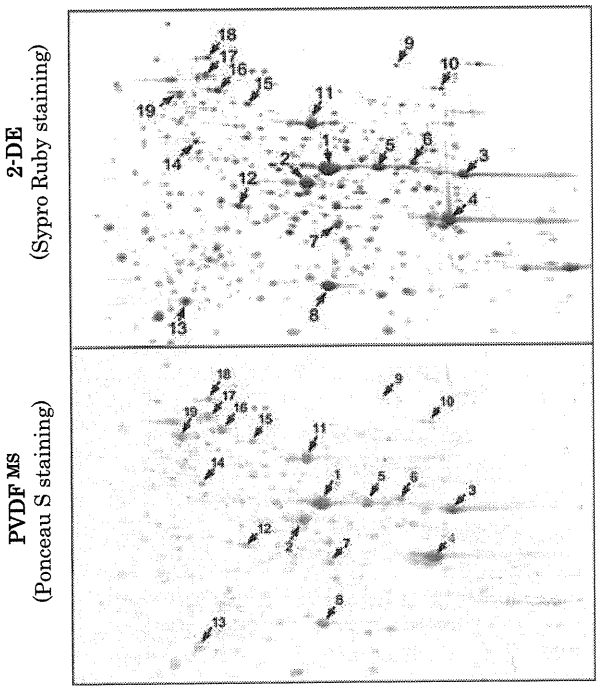

Fig. 3. 2DE patterns of yeast proteins on gel and PVDF membrane. Yeast proteins were separated by 2DE and electroblotted onto a 0.1 μm pore-size PVDF membrane. A total of 19 distinctive proteins were digested on the membrane with trypsin. The digests were analyzed by MALDI-quadrupole ion trap (QIT)/TOF MS and the following proteins were identified: 1, phosphopyruvate hydrase; 2, fructose-bisphosphate aldolase; 3, phosphoglycerate kinase; 4, glyceraldehyde-3-phosphate dehydrogenase; 5, alcohol dehydrogenase; 6 and 7, enolase; 8, triosephosphate isomerase; 9, 5-methyltetrahydropteroyl triglutamate-homocysteine *S*-methyltransferase; 10, transketolase; 11, pyruvate decarboxylase; 12, inorganic pyrophosphatase; 13, thiol-specific antioxidant protein; 14, H^+-transporting two-sector ATPase; 15, magnesium-activated aldehyde dehydrogenase; 16, heat shock protein SSB1; 17, DnaK-type molecular chaperone SSC1 precursor, 18; heat shock protein MSI3; and 19, heat shock protein HSP60 precursor.

complicated processing, such as surface grinding and chemical modifications, to activate the surface. Therefore, it would be ideal if membrane filters, such as PVDF, could be used instead of DLC plates.

Concluding remarks

Various biochemical characteristics of proteins can be analyzed, after separation by gel electrophoresis and electroblotting onto PVDF membranes. This technique, in which the electroblotted proteins are subjected to on-membrane protease digestion and the resultant peptides are analyzed directly by MALDI-MS on the membranes, has been studied and improved for more than 20 years and is practically useful. Developing novel blotting filters, blotting techniques and mass spectrometers will be particularly important for more efficient and effective electroblotting and MS analyses.

Acknowledgement

This work was partially supported by Special Coordination Fund for Promoting Science and Technology 'Creation and Innovation Centers for Advanced Interdisciplinary'.

References

1 Wolters DA, Washburn MP & Yates JR III (2001) An automated multidimensional protein identification technology for shotgun proteomics. *Anal Chem* **73**, 5683–5690.
2 Sutton CW, Pemberton KS, Cottrell JS, Corbett JM, Wheeler CH, Dunn MJ & Pappin DJ (1995) Identification of myocardial proteins from two-dimensional gels by peptide mass fingerprinting. *Electrophoresis* **16**, 308–316.
3 Gundry RL, White MY, Murray CI, Kane LA, Fu Q, Stanley BA & Van Eyk JE (2009) Preparation of proteins and peptides for mass spectrometry analysis in a bottom-up proteomics workflow. *Curr Protoc Mol Biol* **88**, 10.25.1–10.25.23.
4 Perkins DN, Pappin DJ, Creasy DM & Cottrell JS (1999) Probability-based protein identification by searching sequence databases using mass spectrometry data. *Electrophoresis* **20**, 3551–3567.
5 O'Farrell PH (1975) High resolution two-dimensional electrophoresis of proteins. *J Biol Chem* **250**, 4007–4021.
6 Klose J (1975) Protein mapping by combined isoelectric focusing and electrophoresis of mouse tissues. A novel approach to testing for induced point mutations in mammals. *Humangenetik* **26**, 231–243.
7 Jungblut PR, Holzhütter HG, Apweiler R & Schlüter H (2008) The speciation of the proteome. *Chem Cent J* **18**, 2–16.
8 Kinoshita E, Kinoshita-Kikuta E & Koike T (2009) Separation and detection of large phosphoproteins using Phos-tag SDS-PAGE. *Nat Protoc* **4**, 1513–1521.
9 Kimura Y, Nagata K, Suzuki N, Yokoyama R, Yamanaka Y, Kitamura H, Hirano H & Ohara O (2010) Characterization of multiple alternative forms of heterogeneous nuclear ribonucleoprotein K by phosphate-affinity electrophoresis. *Proteomics* **10**, 3884–3895.
10 Camacho-Carvajal MM, Wollscheid B, Aebersold R, Steimle V & Schamel WW (2004) Two-dimensional Blue native/SDS gel electrophoresis of multi-protein

complexes from whole cellular lysates: a proteomics approach. *Mol Cell Proteomics* **3**, 176–182.
11 Kondo T & Hirohashi S (2006) Application of highly sensitive fluorescent dyes (CyDye DIGE Fluor saturation dyes) to laser microdissection and two-dimensional difference gel electrophoresis (2D-DIGE) for cancer proteomics. *Nat Protoc* **1**, 2940–2956.
12 Morita A, Miyagi E, Yasumitsu E, Kawasaki H, Hirano H & Hirahara F (2006) Proteomic search for potential diagnostic markers and therapeutic targets for ovarian clear cell adenocarcinoma. *Proteomics* **6**, 5880–5890.
13 Kamita M, Kimura Y, Ino Y, Kamp RM, Polavoda B, Sherman F & Hirano H (2011) N^{α}-Acetylation of yeast ribosomal proteins : identification by 2D-DIGE MS/MS and analysis of the effect on proteins synthesis. *J Proteomics* **74**, 431–441.
14 Towbin H, Staehelin T & Gordon J (1979) Electrophoretic transfer of proteins from polyacrylamide gels to nitrocellulose sheets: procedure and some applications. *Proc Natl Acad Sci USA* **76**, 4350–4354.
15 Kaufmann H, Bailey JE & Fussenegger M (2001) Use of antibodies for detection of phosphorylated proteins separated by two-dimensional gel electrophoresis. *Proteomics* **1**, 194–199.
16 Packer NH, Pawlak A, Kett WC, Gooley AA, Redmond JW & Williams KL (1997) Proteome analysis of glycoforms: a review of strategies for the microcharacterisation of glycoproteins separated by two-dimensional polyacrylamide gel electrophoresis. *Electrophoresis* **18**, 452–460.
17 Vandekerckhove J, Bauw G, Puype M, Van Damme J & Van Montagu M (1985) Protein-blotting on Polybrene-coated glass-fiber sheets. A basis for acid hydrolysis and gas-phase sequencing of picomole quantities of protein previously separated on sodium dodecyl sulfate/polyacrylamide gel. *Eur J Biochem* **152**, 9–19.
18 Aebersold RH, Teplow DB, Hood LE & Kent SB (1986) Electroblotting onto activated glass. High efficiency preparation of proteins from analytical sodium dodecyl sulfate-polyacrylamide gels for direct sequence analysis. *J Biol Chem* **261**, 4229–4238.
19 Matsudaira P (1987) Sequence from picomole quantities of proteins electroblotted onto polyvinylidene difluoride membranes. *J Biol Chem* **262**, 10035–10038.
20 Eckerskorn C, Strupat K, Karas M, Hillenkamp F & Lottspeich F (1992) Mass spectrometric analysis of blotted proteins after gel electrophoretic separation by matrix-assisted laser desorption/ionization. *Electrophoresis* **13**, 664–665.
21 Strupat K, Karas M, Hillenkamp F, Eckerskorn C & Lottspeich F (1994) Matrix-assisted laser desorption ionization mass spectrometry of proteins electroblotted after polyacrylamide gel electrophoresis. *Anal Chem* **66**, 464–470.
22 Blackledge JA & Alexander AJ (1995) Polyethylene membrane as a sample support for direct matrix-assisted laser desorption/ionization mass spectrometric analysis of high mass proteins. *Anal Chem* **67**, 843–848.
23 Schreiner M, Strupat K, Lottspeich F & Eckerskorn C (1996) Ultraviolet matrix assisted laser desorption ionization-mass spectrometry of electroblotted proteins. *Electrophoresis* **17**, 954–961.
24 Eckerskorn C, Strupat K, Schleuder D, Hochstrasser D, Sanchez J, Lottspeich F & Hillenkamp F (1997) Analysis of proteins by direct-scanning infrared- MALDI mass spectrometry after 2D-PAGE separation and electroblotting. *Anal Chem* **69**, 2888–2892.
25 Patterson SD (1995) Matrix-assisted laser-desorption/ionization mass spectrometric approaches for the identification of gel-separated proteins in the 5–50 pmol range. *Electrophoresis* **16**, 1104–1114.
26 Bunai K, Nozaki M, Hamano M, Ogane S, Inoue T, Nemoto T, Nakanishi H & Yamane K (2003) Proteomic analysis of acrylamide gel separated proteins immobilized on polyvinylidene difluoride membranes following proteolytic digestion in the presence of 80% acetonitrile. *Proteomics* **3**, 1738–1749.
27 Methogo RM, Dufresne-Martin G, Leclerc P, Leduc R & Klarskov K (2005) Mass spectrometric peptide fingerprinting of proteins after Western blotting on polyvinylidene fluoride and enhanced chemiluminescence detection. *J Proteome Res* **4**, 2216–2224.
28 Pham VC, Henzel WJ & Lill JR (2005) Rapid on-membrane proteolytic cleavage for Edman sequencing and mass spectrometric identification of proteins. *Electrophoresis* **26**, 4243–4251.
29 Chang CY, Liao HK, Juo CG, Chen SH & Chen YJ (2006) Improved analysis of membrane protein by PVDF-aided, matrix-assisted laser desorption/ionization mass spectrometry. *Anal Chim Acta* **556**, 237–246.
30 Luque-Garcia JL, Zhou G, Sun TT & Neubert TA (2006) Use of nitrocellulose membranes for protein characterization by matrix-assisted laser desorption/ionization mass spectrometry. *Anal Chem* **78**, 5102–5108.
31 Schleuder D, Hillenkamp F & Strupat K (1999) IR-MALDI-mass analysis of electroblotted proteins directly from the membrane: comparison of different membranes, application to on-membrane digestion, and protein identification by database searching. *Anal Chem* **71**, 3238–3247.
32 Sloane AJ, Duff JL, Wilson NL, Gandhi PS, Hill CJ, Hopwood FG, Smith PE, Thomas ML, Cole RA & Packer NH (2002) High throughput peptide mass fingerprinting and protein macroarray analysis using chemical printing strategies. *Mol Cell Proteomics* **1**, 90–99.
33 Kimura S, Kameyama A, Nakaya S, Ito H & Narimatsu H (2007) Direct on-membrane glycoproteomic approach using MALDI-TOF mass spectrometry

coupled with microdispensing of multiple enzymes. *J Proteome Res* **6**, 2488–2494.
34 Nakanishi T, Ohtsu I, Furuta M, Ando E & Nishimura O (2005) Direct MS/MS analysis of proteins blotted on membranes by a matrix-assisted laser desorption/ionization-quadrupole ion trap-time-of-flight tandem mass spectrometer. *J Proteome Res* **4**, 743–747.
35 Nakanishi T, Ando E, Furuta M, Tsunasawa S & Nishimura O (2007) Direct on-membrane peptide mass fingerprinting with MALDI-MS of tyrosine-phosphorylated proteins detected by immunostaining. *J Chromatogr B Analyt Technol Biomed Life Sci* **847**, 24–29.
36 Chen SH, Liao HK, Chang CY, Juo CG, Chen JH, Chan SI & Chen YJ (2007) Targeted protein quantitation and profiling using PVDF affinity probe and MALDI-TOF MS. *Proteomics* **7**, 3038–3050.
37 Ino Y, Kazamaki R & Hirano H (2010) *On-Membrane Identification of Gel-Resolved Proteins by MALDI-MS, Methods in Protein Biochemistry*, Tschesche H (ed.), De Gruyter, Berlin, in press.
38 Iwafune Y, Tan JZ, Ino Y, Okayama A, Ishigaki Y, Saito K, Suzuki N, Arima M, Oba M, Kamei S *et al.* (2007) On-chip identification and interaction analysis of gel-resolved proteins using a diamond-like carbon-coated plate. *J Proteome Res* **6**, 2315–2322.
39 Hirano H (1989) Microsequence analysis of winged bean seed proteins electroblotted from two-dimensional gel. *J Protein Chem* **8**, 115–130.

JOURNAL OF PROTEOMICS 74 (2011) 431–441

available at www.sciencedirect.com

ScienceDirect

www.elsevier.com/locate/jprot

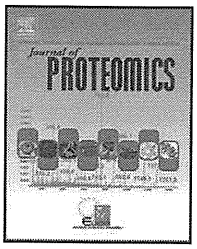

N^{α}-Acetylation of yeast ribosomal proteins and its effect on protein synthesis

Masahiro Kamita[a], *Yayoi Kimura*[a], *Yoko Ino*[a], *Roza M. Kamp*[b], *Bogdan Polevoda*[c], *Fred Sherman*[c], *Hisashi Hirano*[a,*]

[a]*Graduate School of Nanobioscience, Yokohama City University, Suehiro 1-7-29, Tsurumi, Yokohama 230-0045, Japan*
[b]*University of Applied Science and Technology, 13347 Berlin, Germany*
[c]*Department of Biochemistry and Biophysics, University of Rochester Medical Center, Rochester, NY 14642, USA*

ARTICLE INFO

Article history:
Received 21 November 2010
Accepted 15 December 2010
Available online 22 December 2010

Keywords:
N^{α}-Acetylation
Ribosome
Ribosomal protein
2D-DIGE

ABSTRACT

N^{α}-Acetyltransferases (NATs) cause the N^{α}-acetylation of the majority of eukaryotic proteins during their translation, although the functions of this modification have been largely unexplored. In yeast (*Saccharomyces cerevisiae*), four NATs have been identified: NatA, NatB, NatC, and NatD. In this study, the N^{α}-acetylation status of ribosomal protein was analyzed using NAT mutants combined with two-dimensional difference gel electrophoresis (2D-DIGE) and mass spectrometry (MS). A total of 60 ribosomal proteins were identified, of which 17 were N^{α}-acetylated by NatA, and two by NatB. The N^{α}-acetylation of two of these, S17 and L23, by NatA was not previously observed. Furthermore, we tested the effect of ribosomal protein N^{α}-acetylation on protein synthesis using the purified ribosomes from each NAT mutant. It was found that the protein synthesis activities of ribosomes from NatA and NatB mutants were decreased by 27% and 23%, respectively, as compared to that of the normal strain. Furthermore, we have shown that ribosomal protein N^{α}-acetylation by NatA influences translational fidelity in the presence of paromomycin. These results suggest that ribosomal protein N^{α}-acetylation is necessary to maintain the ribosome's protein synthesis function.

1. Introduction

Methionine cleavage and N^{α}-acetylation are two common protein N-terminal modifications [1,2]. A majority of experimentally characterized eukaryotic proteins are N-terminally acetylated by N^{α}-acetyltransferases (NATs) during their translation from mRNA [3]. In yeast (*Saccharomyces cerevisiae*), approximately 57% of proteins are predicted to have an N^{α}-acetyl group, while the corresponding figure for mammalian proteins is about 84% [4]. The N^{α}-acetylation is catalyzed by NATs that contain catalytic subunits homologous to the GNAT family of acetyltransferase [5]. In yeast, four NATs have been identified, NatA, NatB, NatC, and NatD, which are composed of the following catalytic and auxiliary subunits: Ard1p and Nat1p for NatA; Nat3p and Mdm20p for NatB; and Mak3p, Mak10p, and Mak31p for NatC [6]. A recent study has shown NatD to consist of only a catalytic subunit: Nat4p [7]. The deletion of NATs induces various phenotypes. The NatA deletion mutant exhibits defects in sporulation, salt sensitivity, mating efficiency, and the ability to enter G0. The NatB deletion mutant shows increased osmotic sensitivity, decreased utilization of non-fermentable carbon sources, reduced mating efficiency, inability to form functional actin filaments, defects in mitochondrial and vacuolar inheritance, random polarity, increased sensitivity to the anti-mitotic drugs, and increased susceptibility to a number of DNA damaging agents. The NatC deletion mutant shows a decreased growth on YPG medium at 37 °C, although growth on YPD medium at 30 °C is nearly normal [6].

* *Corresponding author.* Tel.: +81 45 508 7439; fax: +81 45 508 7667.
E-mail address: hirano@yokohama-cu.ac.jp (H. Hirano).

1874-3919/$ – see front matter © 2010 Elsevier B.V. All rights reserved.
doi:10.1016/j.jprot.2010.12.007

Despite the wide occurrence of protein N^{α}-acetylation, it is unknown how many proteins require N^{α}-acetylation for function. For instance, the N^{α}-acetylation of Orc1p and Sir3p was shown to be necessary for transcriptional silencing in yeast [8,9]. Also, the N^{α}-acetylation of the killer viral coat protein Gag by NatC is required for assembly and maintenance of the L-A dsRNA viral particle in yeast [10]. Unacetylated actin and tropomyosin have a number of defects *in vivo* and *in vitro*, although the mutants are viable [11]. While the N^{α}-acetylation of ribosomal proteins has been known for decades [12–14], the role of N^{α}-acetylation in translation has not been determined.

The ribosome is a large ribonucleoprotein complex that synthesizes proteins in the cytoplasm. The core of the structure, as well as many of the ribosomal functions, is highly conserved between eukaryotes and prokaryotes [15]. In yeast, the ribosome consists of two subunits, the large (60S) and small (40S) subunits. The 60S subunit is composed of three ribosomal RNAs (rRNAs) and 46 ribosomal proteins, whereas the 40S subunit is composed of one rRNA and 32 ribosomal proteins [16,17]. The ribosome translates mRNA sequences into the corresponding amino acids and links them together to synthesize proteins. There are four stages of protein synthesis: initiation, elongation, termination, and recycling [18]. The 60S subunit polymerizes the polypeptide chain during the elongation phase. The 40S subunit is associated with mRNA tracks, the tRNA binding site, and is instrumental in selecting an aminoacyl-tRNA that complements the bound mRNA codon [16]. Although the rRNAs basically catalyze translation of mRNA and peptide bond formation, ribosomal proteins have been shown to play several important roles in protein synthesis, including determining the conformation of the ribosome structure and binding the various translational factors [19].

The ribosomal proteins undergo a variety of post-translational modifications including phosphorylation, methylation, glycosylation, and N^{α}-acetylation (co-translational). The post-translational modifications are thought to affect the ribosomal function. For example, Ruvinsky et al. reported that phosphorylation of ribosomal protein S6 controls cell size and glucose homeostasis [20]. Phosphorylation of ribosomal protein P1A exerts an effect on the hetero-oligomerization process [21]. Additionally, it is known that arginine methylation of ribosomal protein S10 regulates ribosome biogenesis [22], and arginine methylation of ribosomal proteins S3 affects ribosome assembly [23]. Glycosylation of ribosomal proteins is required for aggregation of untranslated messenger ribonucleoproteins into stress granules [24]. Clearly, modifications of ribosomal proteins are important for protein synthesis. However, the effect of N^{α}-acetylation of ribosomal proteins, and therefore changes of ribosome function remain unknown.

In this study, we comprehensively analyzed ribosomal protein N^{α}-acetylation using NAT mutants combined with two-dimensional difference gel electrophoresis (2D-DIGE) and mass spectrometry (MS). These analyses led to the identification of 19 ribosomal proteins acetylated by NatA and NatB. Subsequently, we investigated the effect of ribosomal protein N^{α}-acetylation on protein synthesis using the NatA deletion mutant.

2. Material and methods

2.1. Yeast strains and media

The following strains were used in this study: the normal strain, B-8032 (MATα *ura3-52 CYC1-963 cyc7-67 lys5-10*); the *nat1* mutant, B-8360 (MATα *nat1::URA3 ura3-52 CYC1-963 cyc7-67 lys5-10*); the *mak3* mutant, B-9074 (MATα *mak3::URA3 CYC1-963 cyc7-67 lys5-10*); and the *nat3* mutant, B-11974 (MATα *nat3::kanMX2 CYC1-963 cyc7-67 lys5-10*).

The YPD medium [2% (w/v) glucose, 2% (w/v) pepton, and 1% (w/v) yeast extract] was used for growing yeast. To purify 80S ribosomes, the yeast cells were cultured in the YPD medium at 30 °C. The cells were grown to the mid log phase, an absorbance of ~2 A_{600} U/ml, and harvested by centrifugation, washed once with deionized water and stored at −80 °C. For the 10-fold serial dilution assays, freshly grown yeast colonies were suspended in deionized water, and 1/10 dilutions, starting at an optical density of 0.1 at 600 nm, were spotted on a YPD plate or a YPD plate containing antibiotics. The plates were then incubated at 20, 30, or 37 °C for 3 to 4 days.

2.2. Purification of 80S ribosomes and ribosomal proteins

Purification of yeast ribosomes was performed as described by Ulrich A et al. with some modifications [25]. Briefly, the stored yeast cells were resuspended in the extraction buffer [20 mM HEPES-KOH pH 7.0, containing 5 mM Mg-acetate$_2$, 2 mM spermidine, 0.1 mM EGTA, 10 mM 2-mercaptoethanol, 10% (v/v) glycerol, and 0.1 mM PMSF]. Glass beads were added and the cells broken by vigorous vortex shaking. The homogenate was centrifuged at 20,000 ×*g* for 30 min at 4 °C. To purify 80S ribosomes, the concentration of KCl in the supernatant was adjusted to 0.4 M while being mixed gently. Thereafter, the supernatant was centrifuged at 65,000 ×*g* for 5 h at 4 °C. The resulting ribosome pellet was then resuspended in the dissociation buffer [20 mM HEPES-KOH pH 7.0, containing 5 mM Mg-(Ac)$_2$, 500 mM K(Ac), 0.1 mM EGTA, 10 mM 2-mercaptoethanol, 10% (v/v) glycerol, and 0.1 mM PMSF] and puromycin and GTP were added to a final concentration of 1 mM each. The mixture was incubated at 30 °C for 30 min. After incubation, the ribosome was pelleted through a 25% (v/v) glycerol cushion in the dissociation buffer at 65,000 ×*g* for 12 h at 4 °C using a swinging bucket rotor. The pellet was resuspended again and then centrifuged at 65,000 ×*g* for 12 h at 4 °C. Finally, the resulting 80S ribosome pellet was resuspended in the reaction buffer [50 mM Tris–HCl pH 7.6 containing 15 mM $MgCl_2$, and 90 mM KCl]. To separate the ribosomal proteins from the rRNA of the ribosome, the resuspended pellet was precipitated with 0.1 volume of 0.1% (w/v) DTT, 0.1 volume of 1 M $MgCl_2$, and 2.5 volume of glacial acetic acid. After incubation on ice for 1 h, the rRNA was removed by centrifugation at 20,000 ×*g* for 10 min. The supernatant was dialyzed against deionized water.

2.3. Gel electrophoresis of rRNAs and ribosomal proteins

The rRNAs (1 μg) were incubated at 65 °C for 2 min in the loading solution [0.1% (w/v) SDS, 5% (v/v) glycerol and BPB],

and subjected to electrophoresis in 0.8% (w/v) agarose gel. The ribosomal proteins (10 μg) were incubated at 65 °C for 10 min in the sample buffer [0.05 M Tris–HCl pH 6.8, containing 2% (w/v) SDS, 5% (v/v) 2-mercaptoethanol, 10% (v/v) glycerol, and BPB] and subsequently separated by SDS-PAGE. On the other hand, two-dimensional electrophoresis (2-DE) was performed using acid-urea gels containing 8 M urea in the first dimension toward the cathode (pH 5.0) at constant 200 V for 800 V h, and SDS-PAGE (14% acrylamide gel) in the second dimension. After 2-DE, proteins were detected by CBB R-250 staining.

2.4. *Two-dimensional difference gel electrophoresis*

For 2D-DIGE, purified ribosomal proteins were minimally labeled with CyDyes (GE Healthcare, Little Calfont, UK) Cy3 and Cy5 according to the manufacturer's protocol. Equal amounts of purified ribosomal proteins from the normal and the mutant strains were labeled with two different dyes, Cy3 for the normal and Cy5 for the mutant strains. The ratio of ribosomal proteins to CyDye was 50 μg to 128 pmol. All labeled samples were combined and dissolved in 20 μl of sample solution [10% (v/v) 2-mercaptoethanol, 10% (v/v) glycerol, 1% (v/v) acetic acid and 8 M urea], and was subjected to 2-DE. The separated proteins were detected using Typhoon 9400 (GE Healthcare).

2.5. *Protein identification by mass spectrometric analysis*

After electrophoresis, protein spots were cut from the gels, destained three times with destaining solution [50 mM NH_4HCO_3/60% ACN], and digested with trypsin in 50 mM NH_4HCO_3 at 37 °C for 12 h. The tryptic digests were applied to Amicon Ultrafree-MC (0.22 μm) devices and centrifuged at 7000 rpm for 5 min. After filtration, a solution containing 0.02% (v/v) TFA and 0.2% (v/v) formic acid was added to the Amicon Ultrafree-MC tubes and centrifuged again. The resulting peptides were resuspended in 0.3% (v/v) formic acid, and analyzed using an ESI-Linear Ion Trap (LIT)-TOF MS (NanoFrontier LD, Hitachi-High Technologies, Tokyo, Japan) or an ESI-Q-TOF MS (Micromass, Manchester, UK), respectively. For data analysis, the raw MS spectrum was processed using the Hitachi-High Technologies' data processing software or the Micromass' MassLynx software to generate MGF and PKL files, respectively. The obtained MS and MS/MS data were searched against the 6,858 yeast protein sequences of the SWISS-PROT ver. 57.4 database using the MASCOT program, ver. 2.2.04 (Matrix Science, London, UK) to identify proteins. The search parameters were as follows: protease digestion with two missed cleavages permitted, enzyme specificity was set to consider trypsin, propionamidation of cysteine, and oxdation of methionine as variable modifications, and mass tolerance was set to 0.5 Da for the fragment ions and precursor ions. The confidence interval for the MASCOT scores was set to 95% (significance threshold $p<0.05$). Additionally, search results that yielded a MASCOT score of ≥95 or 35 for SDS-PAGE or 2-DE, respectively, were accepted as positive identifications.

2.6. *Poly (U)-dependent poly (Phe) synthesis assay*

The 80S ribosomes (0.3 A_{260}U) from the normal and the mutant strains were incubated in 25 μl of an assay mixture containing 50 μg of S-100 fraction, which was purified from the normal strain, 15 μg of polyuridylic acid, 25 μg of tRNA, [^{14}C]-phenylalanine, 0.5 mM GTP, 1 mM ATP, 2 mM phosphocreatine, and 40 μg/ml creatine phosphokinase in 50 mM Tris–HCl pH 7.6, 15 mM $MgCl_2$, 90 mM KCl, and 5 mM 2-mercaptoethanol at 30 °C for 30 min. After incubation, samples were precipitated with 10% (w/v) trichloroacetic acid (TCA) and boiled for 10 min. Subsequently, the samples were placed on ice for 10 min and filtered through glass fiber filters. The filters were washed twice with 10% (w/v) TCA. After air-drying, the insoluble proteins were resuspended in 10% (w/v) TCA and the radioactivity was measured using a liquid scintillation counter.

2.7. *Polysome profiles*

Yeast cells were grown to a mid log phase in the YPD medium. The cells were harvested in the presence of 100 μg/ml cycloheximide for 10 min. Preparation of yeast extracts was carried out by glass bead disruption in 10 mM Tris–HCl pH 7.4, containing 100 mM NaCl, 30 mM $MgCl_2$, and 100 μg/ml cycloheximide. A 200 μl sample of lysate, corresponding to 8 A_{260} U, was applied to a 7–47% linear sucrose gradient that was prepared in 50 mM Tris–acetate pH 7.0, containing 50 mM NH_4Cl, 30 mM $MgCl_2$ and 1 mM DTT for 2.5 h at 38,200 rpm (Beckman, SW40Ti). After centrifugation, fractions were collected from top to bottom with continuous A_{254} monitoring.

2.8. *Translational fidelity assay*

The reporter assay described by Liang et al. was performed with slight modifications [26]. Briefly, a 366 bp PCR fragment containing the Protein A gene was amplified from the common TAP tag. To create the gene encoding the FLAG tag, which is immediately downstream from the stop codon gene of protein A, the first PCR fragment was used as a template for the second PCR. The created PCR fragment was inserted into the KpnI and XbaI restriction site in the plasmid pAUR123. The construct was transformed into both the normal strain and the *nat1* mutant. The transformed cells were disrupted using YPER buffer (Pierce, Rockford, IL, USA) and glass beads. Cell extracts were centrifuged at 20,000 ×*g* for 10 min at 4 °C and supernatants analyzed by SDS-PAGE. The separated proteins were transferred to a polyvinylidene difluoride (PVDF) membrane and the protein A peptide on the membrane was detected with anti-peroxidase antibody. The membrane was incubated with ECL plus (GE Healthcare) and the positive signals were detected using an LAS4000 illuminator (Fuji Film, Tokyo, Japan).

3. Results

3.1. *Ribosome purification and ribosomal protein identification by two-dimensional electrophoresis*

In this study, we purified the 80S ribosomes from the normal yeast strain and the NAT mutants. To check the quality of the purified 80S ribosomes, rRNAs and ribosomal proteins were separated by standard gel electrophoresis (Fig. 1A). As shown in Fig. 1A, sharp bands of 25S and 18S rRNAs were detected, while no

smeared band was detected; this shows that intact 80S ribosomes were purified, with no degradation incurred during purification. Simultaneously, the ribosomal proteins of the 80S ribosomes from the normal strain and the NAT mutants were separated by SDS-PAGE and detected by CBB staining (Fig. 1B). It should be noted that CBB-stained ribosomal protein gel images from the normal strain and the NAT mutants were identical. Then, gel-separated protein bands were in gel-digested by trypsin and the resulting peptides were analyzed by MS/MS to identify the proteins (Supplementary Table 1). A total of 50 ribosomal proteins were identified, but no non-ribosomal proteins were found, indicating that the ribosomes were highly purified.

Next, the ribosomal proteins were separated using 2-DE and detected by CBB staining (Fig. 1C). A total of 59 protein spots were detected on the 2-DE gel. These proteins were in gel-digested with trypsin, and the resultant peptides were analyzed by MS/MS to identify 60 ribosomal proteins (Fig. 1C and Supplementary Table 2). Interestingly, ribosomal proteins S5 (spots 5 and 6) and S10 (spots 54, 55, and 56) were identified in more than two spots having different isoelectric points, suggesting that these ribosomal proteins may be modified with a modification group such as phosphate.

3.2. *Identification of N^{α}-acetylated ribosomal proteins*

To identify which of the NATs acetylates which ribosomal proteins, we analyzed the ribosomal proteins in the normal strain and the NAT mutants using 2D-DIGE, and found that

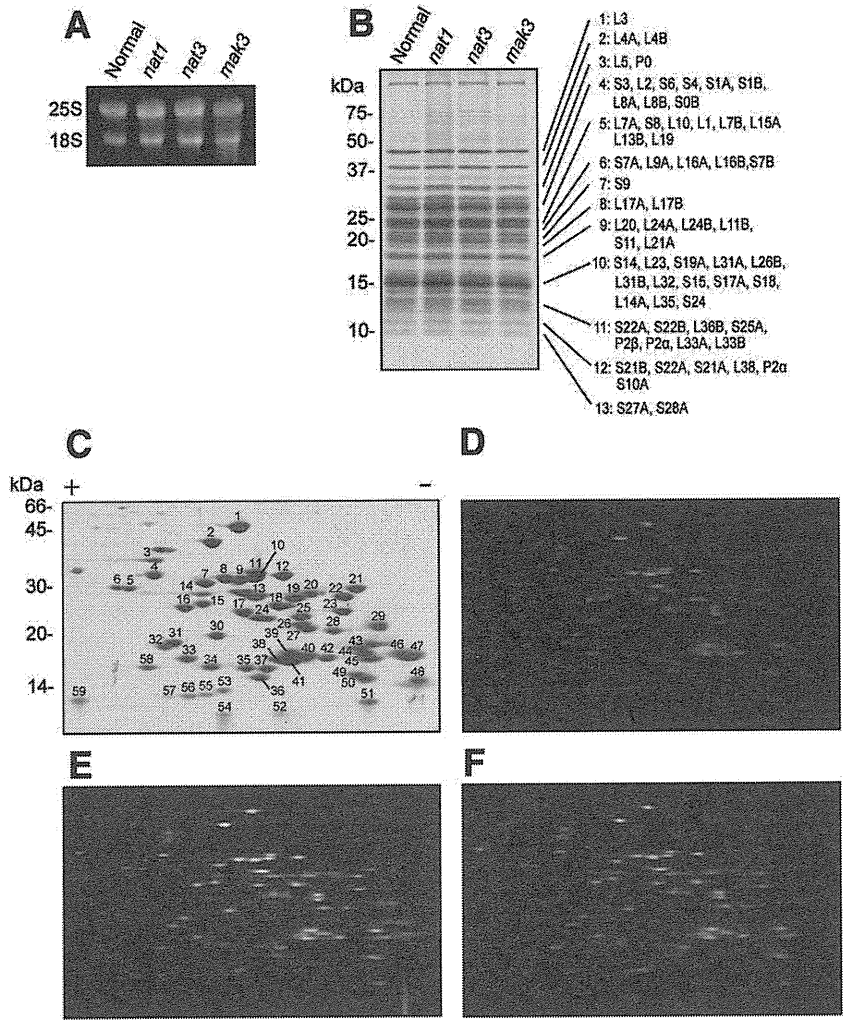

Fig. 1 – Analysis of rRNAs and N^{α}-acetylated ribosomal proteins by 2D-DIGE. (A) Purified rRNA from yeast 80S ribosomes was separated by agarose gel electrophoresis and stained with ethidium bromide. (B) Purified ribosomal proteins from yeast 80S ribosomes were separated by SDS-PAGE and stained with CBB R-250. The details of MS data using an ESI-LIT-TOF MS was shown in Supplementary Table 1. (C) Purified ribosomal proteins from yeast 80S ribosomes were separated by 2-DE using acid-urea electrophoresis in the first dimension and SDS-PAGE in the second dimension and stained with CBB R-250. Protein spots identified by an ESI-Q-TOF-MS are numbered and their details were indicated in Supplementary Table 2. (D–F) Identification of the N^{α}-acetylated ribosomal proteins from the *nat1*, *nat3*, and *mak3* mutants, respectively. Equal amounts of purified ribosomal proteins from the normal strain and the NAT mutant were labeled with Cy3 and Cy5 respectively. The Cy-labeled ribosomal proteins from the two strains were separated on the same 2-DE gel and the Cy3- and Cy5-images were compared. The N^{α}-acetylated ribosomal proteins are shown in Table 1.

Table 1 – N^{α}-Acetylation of ribosomal proteins.

Subunit	Protein	MW (kDa) [a]	pI [a]	2-DE [b]	TOF-MS [c]	DIGE	NAT
60S	P0	33.7	4.6	–	–	–	–
	P1 A/B	10.9/10.6	3.6/3.7	–	●/–	–	–
	P2 A/B	10.7/11.1	3.8/3.9	–	○/○	–	–
	L1 A/B [d]	24.5/24.5	9.7/9.7	–	●/●	●/●	NatA
	L2 A/B [d]	27.4/27.4	11.1/11.1	○/–	–	○/○	–
	L3	43.7	10.3	○	–	○	–
	L4 A/B	39.0/39.0	10.6/10.6	●/–	–	●/●	NatA
	L5	33.7	6.4	–	–	○	–
	L6 A/B	19.9/20.0	10.1/10.1	–	●/–	○/○	–
	L7 A/B	27.6/27.7	10.2/10.2	○/–	○/–	○/○	–
	L8 A/B	28.1/28.1	10.0/10.0	○/–	○/–	○/○	–
	L9 A/B	21.6/21.7	9.7/10.5	–	–	○/–	–
	L10	25.4	10.8	–	○	–	–
	L11 A/B	19.7/19.7	9.9/9.9	●	●/●	●/●	NatA
	L12 A/B [d]	17.8/17.8	9.4/9.4	–	–	○/○	–
	L13 A/B	22.5/22.5	11.2/11.7	–	–	○/–	–
	L14 A/B	15.2/15.2	10.4/11.6	–	●/–	●/–	NatA
	L15 A/B [d]	24.4/24.4	11.4/12.0	○/–	–	○/–	–
	L16 A/B	22.2/22.2	10.5/10.5	●/●	–/●	●/●	NatA
	L17 A/B	20.5/20.5	10.9/10.9	–	○/–	○/○	–
	L18 A/B [d]	20.6/20.6	11.7/11.7	–	–	○/○	–
	L19 A/B [d]	21.7/21.7	11.4/11.4	○/–	–	○/○	–
	L20 A/B	20.4/20.4	10.3/10.3	–	–	○/○	–
	L21 A/B	18.2/18.3	10.4/11.2	–	○/–	○/–	–
	L22 A/B	13.7/13.8	5.9/6.0	–	○/–	○/–	–
	L23 A/B [d]	14.5/14.5	10.3/10.3	–	–	●/●	NatA
	L24 A/B	17.6/17.5	11.3/11.4	–	–	○/○	–
	L25	15.7	10.1	○	○	○	–
	L26 A/B	14.2/14.2	11.4/10.5	–	–/○	–/○	–
	L27 A/B	15.5/15.5	10.4/11.2	–	○/–	○/–	–
	L28	16.7	10.5	–	○	○	–
	L29	6.7	12	–	○	–	–
	L30	11.4	9.8	–	○	○	–
	L31 A/B	12.9/13.0	10.0/10.0	–	○/–	○/○	–
	L32	14.8	11.2	–	○	○	–
	L33 A/B	12.1/12.2	11.1/11.1	–	●/–	○/○	–
	L34 A/B	13.6/13.6	11.6/11.6	–	–	–	–
	L35 A/B [d]	13.9/13.9	10.6/10.6	–	–	○/○	–
	L36 A/B	11.1/11.1	12.2/11.6	–	●/ ○	–/○	–
	L37 A/B	9.8/9.7	12.2/12.3	–	–	–	–
	L38	8.8	10.9	–	○	○	–
	L39	6.3	–	–	○	–	–
	L40 A/B [d]	14.5/14.5	10.6/10.6	–	–	–	–
	L41 A/B [d]	3.3/3.3	–	–	–	–	–
	L42 A/B [d]	12.2/12.2	11.4/11.4	–	–/○	–	–
	L43 A/B [d]	10.0/10.0	11.2/11.4	–	–	–	–
40S	S0 A/B	28.0/28.0	4.5/4.5	–	●/–	–	–
	S1 A/B	28.7/28.8	10.0/10.0	●/–	●/–	○/○	NatA
	S2	27.4	10.4	●	●	●	NatA
	S3	26.5	9.4	○	○	○	–
	S4 A/B [d]	29.3/29.3	10.1/10.1	–	○/–	○/○	–
	S5	25	8.6	●	●	●	NatA
	S6 A/B [d]	27.0/27.0	10.4/10.4	–	–	○/○	–
	S7 A/B	21.6/21.6	9.8/9.9	●/–	●/●	●/●	NatA
	S8 A/B [d]	22.5/22.5	10.7/10.7	–	○/–	○/○	–
	S9 A/B	22.4/22.3	10.8/10.1	–	–	–/○	–
	S10 A/B	12.7/12.7	8.7/9.92	–	○/○	○/–	–
	S11 A/B [d]	17.7/17.7	10.8/10.8	–	●/–	●/●	NatA
	S12	15.8	4.5	–	–	–	–
	S13	17	10.4	–	○	○	–
	S14 A/B	14.5/14.6	10.7/11.3	●/–	●/–	●/–	NatA
	S15	16	10.7	–	●	●	NatA
	S16 A/B [d]	15.8/15.8	10.3/10.3	●/–	●/–	●/●	NatA

(continued on next page)

Table 1 (continued)

Subunit	Protein	MW (kDa)[a]	pI[a]	2-DE[b]	TOF-MS[c]	DIGE	NAT
40S	S17 A/B	15.8/15.8	10.5/11.3	–	–	●/–	NatA
	S18 A/B[d]	17.0/17.0	10.3/10.3	–	●/●	●/●	NatA
	S19 A/B	15.9/15.9	9.6/10.5	–	–/○	○/–	–
	S20	13.9	9.5	–	●	●	NatA
	S21 A/B	9.7/9.5	5.8/5.8	–	●/●	●/●	NatB
	S22 A/B	14.6/14.6	9.9/9.9	–	○/–	○/○	–
	S23 A/B[d]	16.0/16.0	11.5/11.5	–	–	–	–
	S24 A/B[d]	15.3/15.3	10.5/10.5	●/–	●/–	●/●	NatA
	S25 A/B	12.0/12.0	10.3/11.1	–	–	○/–	–
	S26 A/B	13.5/13.4	10.8/11.6	–	–	○/–	–
	S27 A/B	8.9/8.9	9.4/9.5	–	○/○	○/–	–
	S28 A/B	7.6/7.6	10.8/11.4	–	●/●	●/–	NatB
	S29 A/B	6.7/6.7	11.1/10.8	–	○/○	–	–
	S30 A/B	7.1/7.1	12.2/12.2	–	○/○	–	–
	S31	17.2	10.7	–	–	–	–
Total	78			18	50	60	

●: N^{α}-Acetylated ribosomal protein. ○: identified ribosomal protein.
[a] The calculated molecular weight and pI of ribosomal proteins were obtained from SWISS-PROT database.
[b] N^{α}-Acetylated ribosomal proteins were identified by 2-DE with an amino acid sequencer (Takakura et al.).
[c] N^{α}-Acetylated ribosomal proteins were identified by MALDI-TOF-MS (Arnold et al.).
[d] These ribosomal proteins A/B are used for duplicated genes that code proteins with identical sequence.

the following 17 ribosomal proteins in the *nat1* mutant were different in electrophoretic mobility from those in the normal strain (Fig. 1D); S2, S5, S7AB, S11, S14A, S15, S16, S17A, S18, S20, and S24 from the 40S subunit and L1, L4AB, L11B, L14A, L16AB, and L23 from the 60S subunit. These ribosomal proteins prepared from the *nat1* mutant had a shift toward the alkaline side of the gel that corresponds to the change in the protein isoelectric point expected from the lack of N^{α}-acetylation of an α-amino group. In addition, in a sample from the *nat3* mutant two ribosomal proteins, S21 and S28, had altered isoelectric points (Fig. 1E). However, no ribosomal proteins from the *mak3* mutant had changed isoelectric points (Fig. 1F). Although N^{α}-acetylation of ribosomal proteins was reported previously [12–14], this is the first time that ribosomal proteins L23 and S17 have been shown to be the substrates of NatA. The identified N^{α}-acetylated ribosomal proteins are listed in Table 1.

3.3. *Effects of the NAT deletion on cell growth*

It is well known that deletions or mutations of ribosomal protein genes influences both cell growth and temperature-sensitivity. We investigated the growth of the NAT mutants in the YPD medium at 30 °C (Fig. 2A). The doubling time was 1.4, 1.7, 4.0 and 1.4 h for the normal strain, *nat1*, *nat3*, and *mak3* mutants, respectively. The growth of the *nat1* and *nat3* mutants was decreased as compared to the normal strain, while the growth of the mak3 mutant remained unaltered, suggesting that the lack of protein N^{α}-acetylation by NatA and NatB affects cell growth. Next, we investigated the temperature sensitivity of the NAT mutants using 10-fold dilution spot assays performed on YPD plates at three different temperatures (20, 30, and 37 °C) (Fig. 2B). Growth of the normal and the NAT mutants was not significantly affected at 30 °C. In contrast, the *nat1* and *nat3* mutants showed slow growth phenotype at 37 °C.

3.4. *Effect of ribosomal protein N^{α}-acetylation on polyU-dependent poly-(Phe) synthesis*

The slower growth of the *nat1* and *nat3* mutants suggests that ribosomal protein N^{α}-acetylation may have an effect on protein synthesis, the most important function of ribosomes. Changes in the structure or function of yeast ribosomes are known to affect cell growth rate at a range of temperatures. In order to study the effect of ribosomal protein N^{α}-acetylation on protein synthesis, we performed polyU-dependent poly-(Phe) synthesis assays (Fig. 2C). The results demonstrated that the protein synthesis activities of 80S ribosomes purified from the *nat1* and *nat3* mutants were decreased by about 27% and 23%, respectively, as compared to the normal ribosomes. Thus, decreased protein synthesis activities in the *nat1* and the *nat3* mutants could be explained by the lack of N^{α}-acetylation of at least two or more ribosomal proteins from the list of 19 identified acetylated ribosomal protein (see above).

3.5. *Effect of the N^{α}-acetylation on polysome formation*

Polysome analysis in sucrose gradient is used to detect possible defects in ribosomal subunit assembly and proper organization of the ribosome chains that may cause protein synthesis alteration. As we observed decreased translation in the *nat1* and the *nat3* mutants it is possible that ribosome assembly or polysome organization is affected in the mutants. Therefore, we fractionated cell extracts from the normal and the NAT mutants in 7–47% sucrose density-gradient (Fig. 2D). Although the *nat1* and *mak3* mutants exhibited polysome profiles similar to the one from the normal strain, the *nat3* mutant clearly showed a defect in 80S ribosome assembly as the corresponding 80S ribosome peak was significantly decreased and 60S subunit peak was abnormally high. While no disruption of the polysome chains was observed, it appears that the altered ratio of 60S subunits to 80S ribosomes is either

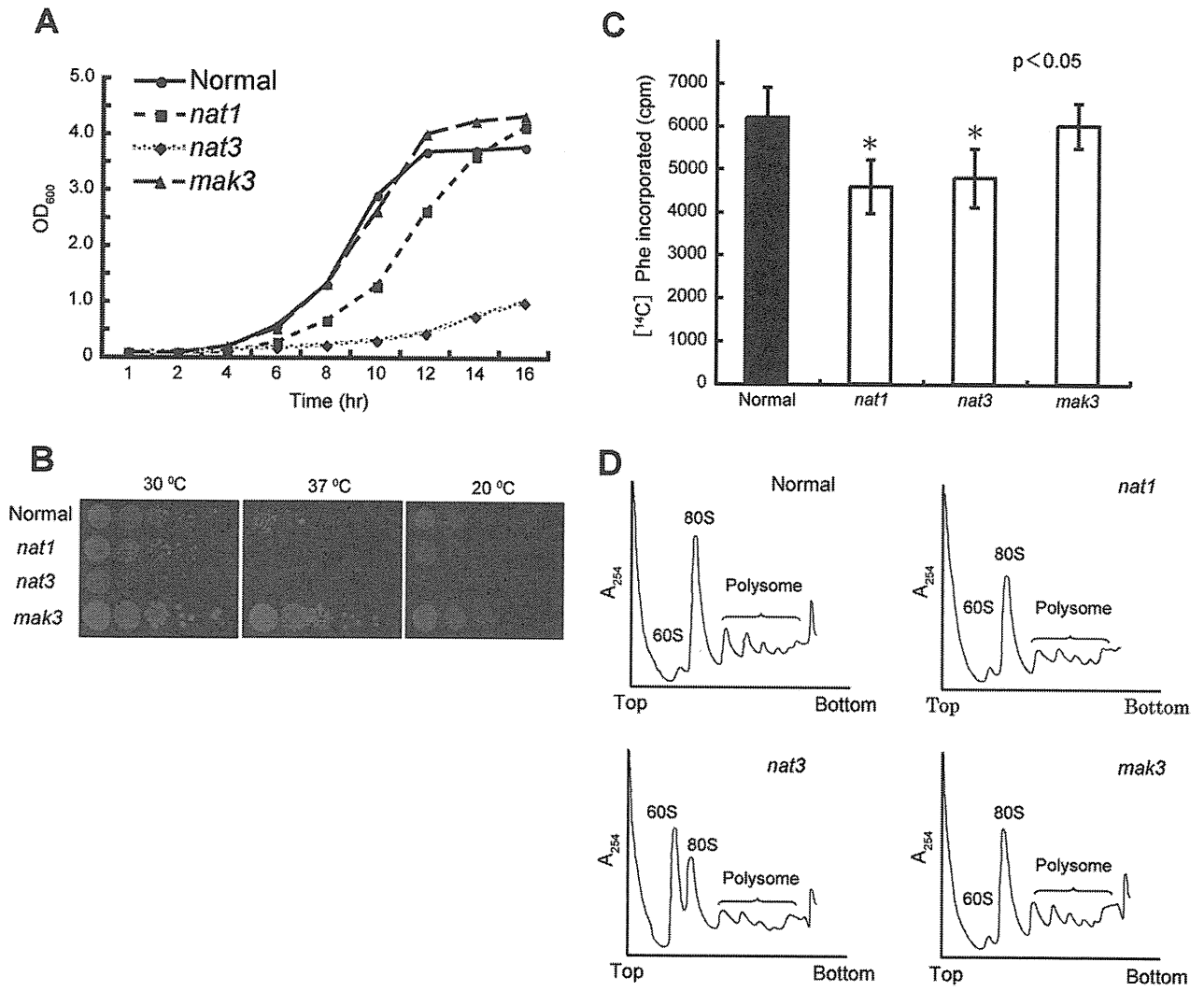

Fig. 2 – The effect of N^{α}-acetylation on cell growth and protein synthesis. (A) Growth curves of the normal strain and the NAT mutants. All strains were cultured in YPD at 30 °C until stationary phase. The absorbance of each culture was measured at 600 nm every 2 h. (B) Effect of three different temperatures (20, 30 and 37 °C) on the growth of the normal strain and the NAT mutants. Freshly grown yeast colonies were suspended in water, and 1/10 dilutions containing the same number of cells were spotted onto YPD plates. Spotted plates were incubated at 20, 30 and 37 °C for 3 to 4 days. (C) Effect of N^{α}-acetylation on polyU-dependent poly (Phe) synthesis. Purified 80S ribosomes from the normal strain and the NAT mutants were added to assay mixtures containing soluble factor S-100 from the normal strain and radioactive Phe residues, and incubated at 30 °C for 30 min. The radioactivity of the insoluble fraction, a measure of the incorporation of radioactive amino acids, was determined by liquid scintillation counter. The value shown in the figure was calculated by subtracting the value of the activity at 0 min. (D) The polysome profiles of the normal strain and the NAT mutants. Cytoplasmic extracts from the normal and the mutant strains were loaded onto 7–47% sucrose gradients, centrifuged, and fractionated. The fractions were collected from the top to the bottom with continuous A_{254} monitoring.

due to a failure to form 80S ribosomes or due to disruption in 40S subunit assembly. Thus, it is possible that decreased protein synthesis activity in the *nat3* mutant is at least in part due to a defect in ribosome assembly, whereas the altered activity in the *nat1* mutant is due to a difference of the fully assembled 80S ribosome.

3.6. *Sensitivity of the nat1 mutant to translation inhibitors*

In order to obtain more data on how NatA ribosomal protein N^{α}-acetylation affects ribosomal functions, we performed 1/10-dilution spot assays using YPD plates containing various antibiotics that bind to the ribosome and inhibit translation (Fig. 3A). We found that neither the normal strain nor the *nat1* mutant was sensitive to puromycin, which is known to cause premature chain termination during translation. However, both of the normal strain and the *nat1* mutant were sensitive to anisomycin and cycloheximide. Anisomycin is a competitive inhibitor of A-site binding that sterically hinders positioning of the acceptor end of A-site tRNA in the peptidyl transferase center (PTC) on the 60S subunit of the ribosome and cycloheximide is known to interfere with the translocation step in protein synthesis by blocking translational elongation. These

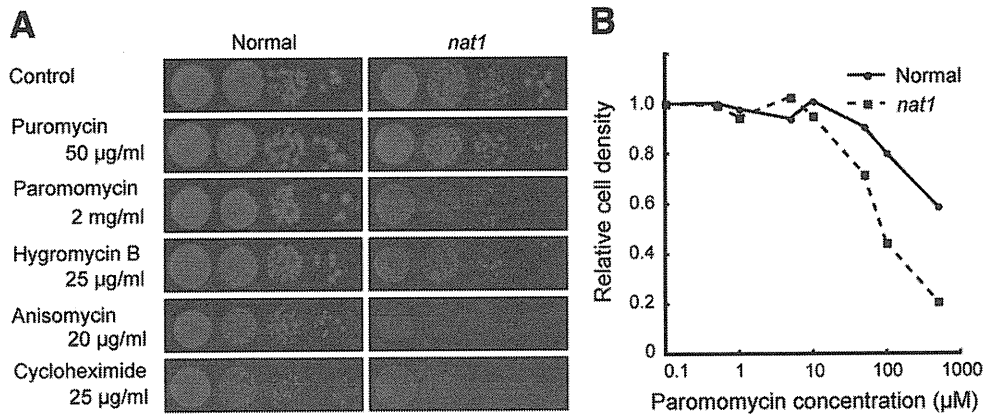

Fig. 3 – The effect of the NatA deletion on sensitivity to translation inhibitors. (A) The effect of various antibiotics on the growth of the normal strain and the *nat1* mutant. Freshly grown yeast colonies were suspended in water, and 1/10 dilutions starting at 0.1 OD_{600} were spotted onto YPD plates containing the indicated antibiotics. Spotted plates were incubated at 30 °C for 4 days. (B) The effect of paromomycin on growth of the normal strain and the *nat1* mutant. Freshly grown yeast colonies were cultured in YPD containing increasing concentrations of antibiotics until the culture without antibiotic reached an OD_{600} of 1–1.5, which was taken as 1.0.

results suggest that N^{α}-acetylation of ribosomal proteins by NatA has no specific effect on translocation or peptidyl transferase activity.

On the other hand, both paromomycin and hygromycin caused a specific decrease in the growth of the *nat1* mutant as compared to the normal strain. Therefore, we examined the effect of various paromomycin concentrations on growth of the *nat1* mutant (Fig. 3B) and found that sensitivity to paromomycin is increasing at higher antibiotic concentrations. Paromomycin is a translational error-inducing antibiotic that binds to the decoding center on the ribosome's 40S subunit and promotes conformational changes affecting formation of the codon–anticodon helix between mRNA and tRNA at the A-site. Thus, it appears that the N^{α}-acetylation of ribosomal proteins by NatA may be required to maintain a proper translational fidelity.

3.7. *The role of ribosomal protein N^{α}-acetylation in translational fidelity*

We investigated the *nat1* mutant's translational fidelity using a bicistronic reporter gene consisting of genes encoding a protein A peptide (14 kDa) and a FLAG peptide (1 kDa) (Fig. 4A). In this assay, if translation is accurate, the 14 kDa peptide is produced. If stop codon readthrough occurs, the 15 kDa peptide (which includes the FLAG tag) is produced. In the normal strain, we analyzed the affect of paromomycin on the level of a readthrough product in a concentration-dependent manner (Fig. 4B). We found that the readthrough product increased with increasing concentrations of paromomycin. Using this construct, we compared translational fidelity between the normal strain and the *nat1* mutant (Fig. 4C). The amount of a stop codon readthrough product in the *nat1* mutant was slightly higher than in the normal strain. Additionally, the level of the readthrough product in the *nat1* mutant was strongly influenced by the addition of paromomycin. Thus, N^{α}-acetylation by NatA is required for optimal translational termination. In addition, our reporter construct is useful for the analysis of translational fidelity in yeast.

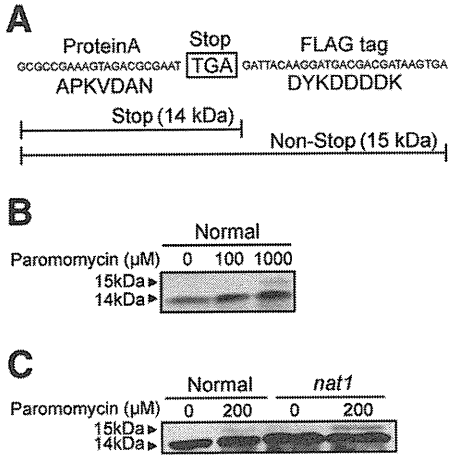

Fig. 4 – The role of ribosomal protein N^{α}-acetylation in translational readthrough activity. (A) The structure of the stop codon readthrough construct used in this study. The 14 kDa protein A fragment is a predominant translation product in the normal strain. The 14 kDa protein A fragment combined with the FLAG tag protein (1 kDa) which resulted in 15 kDa peptide is the mistranslated protein product. (B) Protein production in the normal strain with high concentration of paromomycin induced stop codon readthrough. Cells were grown in YPD containing the indicated concentration of paromomycin. Protein samples were loaded onto 15% SDS-PAGE and detected using Western blot with anti-peroxidase antibody. (C) Comparison of stop codon readthrough activity between the normal strain and the *nat1* mutant.

4. Discussion

Genome sequencing has revealed that yeast contains 137 ribosomal protein genes, encoding 78 unique ribosomal proteins with 59 encoded by duplicate genes [27]. Takakura et al. detected a total of 44 ribosomal proteins in the yeast 80S ribosome by 2-DE using acid-urea gel electrophoresis in the first dimension and SDS-PAGE in the second dimension, and identified 14 ribosomal proteins which were N^{α}-acetylated by NatA using Edman degradation [12]. Arnold et al. found that 30 of the identified 68 ribosomal proteins, including the isoforms, were N-terminally acetylated by NatA, NatB, or NatC using shotgun analysis by MALDI-TOF MS [13]. In the present study, we applied 2D-DIGE and MS/MS to identify the N^{α}-acetylated ribosomal proteins of the yeast 80S ribosome. By these techniques, we detected N^{α}-acetylated proteins and their non-acetylated counterparts as pairs of differently colored spots with slightly different isoelectric points. The numbers of ribosomal proteins and N^{α}-acetylated ribosomal proteins, not including isoforms, were 60 and 19, respectively, showing that we detected 77% of the 78 ribosomal proteins encoded and 83% of the known 69 basic ribosomal proteins (pI > 7). We did not detect the remaining 18 ribosomal proteins by 2D-DIGE, because of low molecular weight (MW < 8000 Da) or isoelectric point (pI < 5).

Nevertheless, this is the first report to describe the use of 2D-DIGE and MS/MS techniques in the differential display analysis of N^{α}-acetylated and non-N^{α}-acetylated ribosomal proteins and we detected more ribosomal proteins and N^{α}-acetylated ribosomal proteins than in the previous studies.

We also investigated the effect of the lack ribosomal protein N^{α}-acetylation on the ribosome function using the NAT mutants. The deletion of *MAK3* (component of NatC) did not affect ribosomal protein N^{α}-acetylation or protein synthesis. In the *nat3* (NatB) mutant, two ribosomal proteins lost the N^{α}-acetyl group, and the protein synthesis activity of purified ribosomes was decreased (Fig. 2). Although the abnormal accumulation of the 60S subunit and lower proportion of the 80S ribosome in the *nat3* mutant might contribute to the low protein synthesis activity of the ribosomes, its mechanism remains unknown. The deletion of *NAT1* (component of NatA) caused the loss of N^{α}-acetylation in 17 ribosomal proteins. The polysome formations of the normal strain and the *nat1* mutant were similar, but the protein synthesis activity of ribosomes purified from the *nat1* mutant was decreased (Fig. 2). In addition, the growth of the *nat1* mutant was decreased on YPD plates, containing the error-inducing antibiotics paromomycin and hygromycin (Fig. 3), and the *nat1* mutant translational read-through activity was increased *in vivo* (Fig. 4). These results are in agreement with the data of Pezza et al. [28].

We assigned the N^{α}-acetylated proteins to the yeast 80S ribosome structure reported by Spahn et al. [29]. Most of the N^{α}-acetylated ribosomal proteins were located around the shoulder, the E-site, or the head on the 40S subunit (Fig. 5). The NatA N^{α}-acetylated ribosomal proteins around the shoulder of the ribosome are conserved between *Escherichia coli* (*E. coli*) and yeast. Among them, *E. coli* ribosomal proteins S4 (yeast ribosomal protein S9 homolog) and S5 (yeast ribosomal protein S2 homolog) contribute to streptomycin resistance [30,31]. Particularly, *E. coli* ribosomal protein S5 is involved in

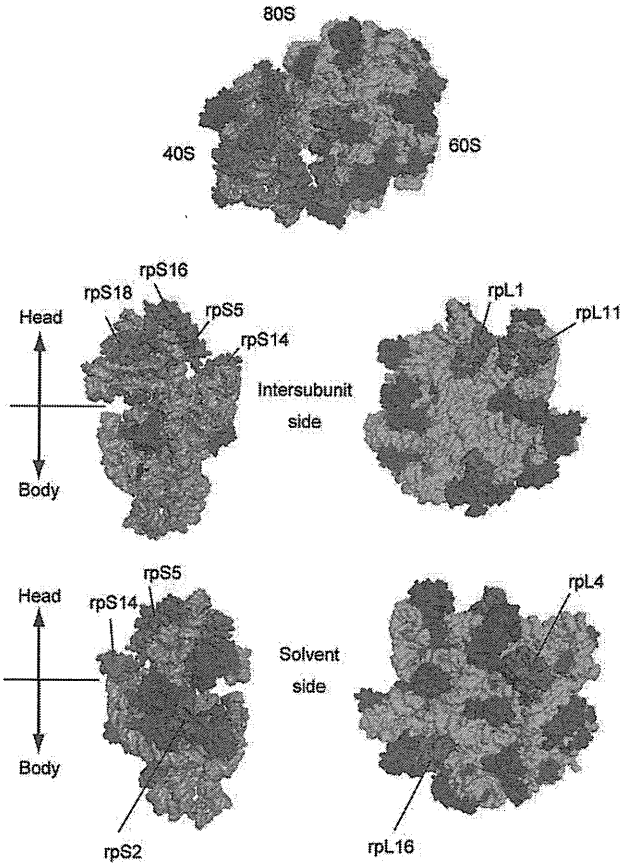

Fig. 5 – Location of NatA N^{α}-acetylated ribosomal proteins on the 80S ribosome structure. The 25S rRNA is in light blue, the 18S rRNA is in green, the non-N^{α}-acetylated ribosomal proteins are in dark blue, and the N^{α}-acetylated ribosomal proteins are in red. The graphic visualization was done with the program PyMol (PDB ID: 1S1H and 1S1I).

tRNA selection and translational fidelity [32]. To determine whether the lack of yeast ribosomal protein S2 N^{α}-acetylation affects translational readthrough, we tested the ribosomal protein S2 mutant with altered N-terminal residue and lacking acetylation. In this experiment, a penultimate serine residue was replaced with tyrosine by mutating the corresponding locus of genomic DNA encoding for S2, resulting in expression of non-N^{α}-acetylated S2 in the mutant. The results show that non-N^{α}-acetylated S2 was not sensitive to paromomycin, suggesting that the N^{α}-acetylation of other ribosomal proteins besides S2 is necessary for translational fidelity in yeast.

The function of the E-site, at which NatA N^{α}-acetylated ribosomal proteins S5 and S14 are located, is to release tRNA and mRNA from the ribosome [33]. The E-site is allosterically coupled to the A-site, and this coupling controls the ability of the ribosome to discriminate between cognate and noncognate tRNAs at the A-site [34]. According to previous reports, the N-terminal domain (~46 amino acids) of yeast ribosomal protein S5 plays an important role in initiation of translation and translational fidelity [35,36]. It is possible that loss of the N^{α}-acetylation of the ribosomal proteins located at the E site contributes to the decreased translational fidelity.

In addition, the N^{α}-acetylated ribosomal proteins S15, S16, S18, and S20 are located at the head of the 40S subunit. There are no reports describing the role of these ribosomal proteins in protein synthesis. However, the present data suggest that the ribosomal proteins located at the ribosome head may be involved in the protein synthesis function as the lack of N^{α}-acetylation of these protein affect protein synthesis.

In yeast, ribosomal proteins L12 and S25 are methylated by N-terminal methyltransferase Tae1p [37]. Interestingly, *TAE1* deletion has similar phenotypes to some of the NatA deletion phenotypes, for example, protein synthesis activity is decreased and paromomycin sensitivity is increased [38]. N-terminal modification causes neutralization of the positive charge on the N-terminal amino group of the protein. Therefore, the lack of N-terminal acetylation and the presence of a positive charge on the N-terminus may affect the interaction between the various components of the ribosome, such as ribosomal proteins, rRNA, and tRNA, causing defects in translation function.

In general, the lack of N^{α}-acetylation can cause any of the following degrees of effects: (*i*) no substantial change of function or stability; (*ii*) partial diminution of function or stability; (*iii*) complete or almost complete loss of function or stability. For example, yeast iso-1-cytochrome *c*, which is normally not N^{α}-acetylated, is not affected by N^{α}-acetylation introduced by mutation of the N-terminal region [5]. An opposite example, the lack of N^{α}-acetylation of the killer viral coat protein Gag causes a 5 to 10-fold reduction of the protein [10]. However, the function or stability of most proteins is less affected by the lack of N^{α}-acetylation, as examined in detail with actin and tropomyosin [11]. The lack of N^{α}-acetylation of actin results in only approximately 50% of the ATPase activation. We wish to emphasize that *act1*-Δ mutants are lethal, as are deletions of genes that encode any essential protein. In this regard, genes encoding ribosomal proteins are essential, as are hundreds of other genes, suggesting that the lack of N^{α}-acetylation of proteins in mutants of NatA, NatB, and NatC cause only partial defects. Also, the concomitant defects in NatA and NatB mutants make it difficult to assign the functions to specific ribosomal proteins.

Supplementary materials related to this article can be found online at doi:10.1016/j.jprot.2010.12.007.

Acknowledgements

This work was supported in part by Special Coordination Funds for Promoting Science and Technology "Creation of Innovation Centers for Advanced Interdisciplinary Research Areas" (to H.H.) and in part by the National Institutes of Health Grant R01 GM12702 (to F.S.).

REFERENCES

[1] Frottin F, Martinez A, Peynot P, Mitra S, Holz RC, Giglione C, et al. The proteomics of N-terminal methionine cleavage. Mol Cell Proteomics 2006;5:2336–49.

[2] Bradshaw RA, Brickey WW, Walker KW. N-terminal processing: the methionine aminopeptidase and N alpha-acetyl transferase families. Trends Biochem Sci 1998;23:263–7.

[3] Gautschi M, Just S, Mun A, Ross S, Rücknagel P, Dubaquié Y, et al. The yeast N(alpha)-acetyltransferase NatA is quantitatively anchored to the ribosome and interacts with nascent polypeptides. Mol Cell Biol 2003;23:7403–14.

[4] Arnesen T, Van Damme P, Polevoda B, Helsens K, Evjenth R, Colaert N, et al. Proteomics analyses reveal the evolutionary conservation and divergence of N-terminal acetyltransferases from yeast and humans. Proc Natl Acad Sci USA 2009;106:8157–62.

[5] Polevoda B, Sherman F. N-terminal acetyltransferases and sequence requirements for N-terminal acetylation of eukaryotic proteins. J Mol Biol 2003;325:595–622.

[6] Polevoda B, Sherman F. Composition and function of the eukaryotic N-terminal acetyltransferase subunits. Biochem Biophys Res Commun 2003;308:1–11.

[7] Polevoda B, Hoskins J, Sherman F. Properties of Nat4, an N (alpha)-acetyltransferase of *Saccharomyces cerevisiae* that modifies N termini of histones H2A and H4. Mol Cell Biol 2009;29:2913–24.

[8] Geissenhöner A, Weise C, Ehrenhofer-Murray AE. Dependence of ORC silencing function on NatA-mediated Nalpha acetylation in *Saccharomyces cerevisiae*. Mol Cell Biol 2004;24: 10300–12.

[9] Wang X, Connelly JJ, Wang CL, Sternglanz R. Importance of the Sir3 N terminus and its acetylation for yeast transcriptional silencing. Genetics 2004;168:547–51.

[10] Tercero JC, Wickner RB. MAK3 encodes an N-acetyltransferase whose modification of the L-A gag NH2 terminus is necessary for virus particle assembly. J Biol Chem 1992;267: 20277–81.

[11] Polevoda B, Cardillo TS, Doyle TC, Bedi GS, Sherman F. Nat3p and Mdm20p are required for function of yeast NatB N^{α}-terminal acetyltransferase and of actin and tropomyosin. J Biol Chem 2003;278:30686–97.

[12] Takakura H, Tsunasawa S, Miyagi M, Warner JR. NH_2-terminal acetylation of ribosomal proteins of *Saccharomyces cerevisiae*. J Biol Chem 1992;267:5442–5.

[13] Arnold RJ, Polevoda B, Reilly JP, Sherman F. The action of N-terminal acetyltransferases on yeast ribosomal proteins. J Biol Chem 1999;274:37035–40.

[14] Lee SW, Berger SJ, Martinović S, Pasa-Tolić L, Anderson GA, Shen Y, et al. Direct mass spectrometric analysis of intact proteins of the yeast large ribosomal subunit using capillary LC/FTICR. Proc Natl Acad Sci USA 2002;99:5942–7.

[15] Nilsson J, Sengupta J, Gursky R, Nissen P, Frank J. Comparison of fungal 80S ribosomes by cryo-EM reveals diversity in structure and conformation of rRNA expansion segments. J Mol Biol 2007;369:429–38.

[16] Dresios J, Panopoulos P, Synetos D. Eukaryotic ribosomal proteins lacking a eubacterial counterpart: important players in ribosomal function. Mol Microbiol 2006;59:1651–63.

[17] Planta RJ, Mager WH. The list of cytoplasmic ribosomal proteins of *Saccharomyces cerevisiae*. Yeast 1998;14:471–7.

[18] Blanchard SC, Cooperman BS, Wilson DN. Probing translation with small-molecule inhibitors. Chem Biol 2010;17: 633–45.

[19] Wilson DN, Nierhaus KH. Ribosomal proteins in the spotlight. Crit Rev Biochem Mol Biol 2005;40:243–67.

[20] Ruvinsky I, Sharon N, Lerer T, Cohen H, Stolovich-Rain M, Nir T, et al. Ribosomal protein S6 phosphorylation is a determinant of cell size and glucose homeostasis. Genes Dev 2005;19:2199–211.

[21] Tchórzewski M, Boguszewska A, Dukowski P, Grankowski N. Oligomerization properties of the acidic ribosomal P-proteins from *Saccharomyces cerevisiae*: effect of P1A protein phosphorylation on the formation of the P1A-P2B hetero-complex. Biochim Biophys Acta 2000;1499:63–73.

[22] Ren J, Wang Y, Liang Y, Zhang Y, Bao S, Xu Z. Methylation of ribosomal protein S10 by protein–arginine methyltransferase 5 regulates ribosome biogenesis. J Biol Chem 2010;285:12695–705.
[23] Shin HS, Jang CY, Kim HD, Kim TS, Kim S, Kim J. Arginine methylation of ribosomal protein S3 affects ribosome assembly. Biochem Biophys Res Commun 2009;385:273–8.
[24] Ohn T, Kedersha N, Hickman T, Tisdale S, Anderson P. A functional RNAi screen links O-GlcNAc modification of ribosomal proteins to stress granule and processing body assembly. Nat Cell Biol 2008;10:1224–31.
[25] Graham John M, David Rickwood. Subcellular fractionation: a practical approach. IRL Press at Oxford University Press; 1997.
[26] Liang XH, Liu Q, Fournier MJ. rRNA modifications in an intersubunit bridge of the ribosome strongly affect both ribosome biogenesis and activity. Mol Cell 2007;28:965–77.
[27] Link AJ, Eng J, Schieltz DM, Carmack E, Mize GJ, Morris DR, et al. Direct analysis of protein complexes using mass spectrometry. Nat Biotechnol 1999;17:676–82.
[28] Pezza JA, Langseth SX, Raupp Yamamoto R, Doris SM, Ulin SP, Salomon AR, et al. The NatA acetyltransferase couples Sup35 prion complexes to the [PSI+] phenotype. Mol Biol Cell 2009;20:1068–80.
[29] Spahn CM, Gomez-Lorenzo MG, Grassucci RA, Jørgensen R, Andersen GR, Beckmann R, et al. Domain movements of elongation factor eEF2 and the eukaryotic 80S ribosome facilitate tRNA translocation. EMBO J 2004;23:1008–19.
[30] Andersson DI, Bohman K, Isaksson LA, Kurland CG. Translation rates and misreading characteristics of rpsD mutants in *Escherichia coli*. Mol Gen Genet 1982;187:467–72.
[31] Piepersberg W, Böck A, Wittmann HG. Effect of different mutations in ribosomal protein S5 of *Escherichia coli* on translational fidelity. Mol Gen Genet 1975;140:91–100.
[32] Ogle JM, Murphy FV, Tarry MJ, Ramakrishnan V. Selection of tRNA by the ribosome requires a transition from an open to a closed form. Cell 2002;111:721–32.
[33] Carter AP, Clemons WM, Brodersen DE, Morgan-Warren RJ, Wimberly BT, Ramakrishnan V. Functional insights from the structure of the 30S ribosomal subunit and its interactions with antibiotics. Nature 2000;407:340–8.
[34] Nierhaus KH. Decoding errors and the involvement of the E-site. Biochimie 2006;88:1013–9.
[35] Galkin O, Bentley AA, Gupta S, Compton BA, Mazumder B, Kinzy TG, et al. Roles of the negatively charged N-terminal extension of *Saccharomyces cerevisiae* ribosomal protein S5 revealed by characterization of a yeast strain containing human ribosomal protein S5. RNA 2007;13:2116–28.
[36] Lumsden T, Bentley AA, Beutler W, Ghosh A, Galkin O, Komar AA. Yeast strains with N-terminally truncated ribosomal protein S5: implications for the evolution, structure and function of the Rps5/Rps7 proteins. Nucleic Acids Res 2010;38: 1261–72.
[37] Webb KJ, Lipson RS, Al-Hadid Q, Whitelegge JP, Clarke SG. Identification of protein N-terminal methyltransferases in yeast and humans. Biochemistry 2010;49:5225–35.
[38] Alamgir M, Eroukova V, Jessulat M, Xu J, Golshani A. Chemical-genetic profile analysis in yeast suggests that a previously uncharacterized open reading frame, YBR261C, affects protein synthesis. BMC Genomics 2008;9:583.